

Inhibitors

Optochemical Control of Therapeutic Agents through Photocatalyzed Isomerization

 Emma E. Watson⁺, Francesco Russo⁺, Dimitri Moreau, and Nicolas Winssinger*

Abstract: A Ru(bpy)₃Cl₂ photocatalyst is applied to the rapid *trans* to *cis* isomerization of a range of alkene-containing pharmacological agents, including combretastatin A-4 (CA-4), a clinical candidate in oncology, and resveratrol derivatives, switching their configuration from inactive substances to potent cytotoxic agents. Selective *in cellulo* activation of the CA-4 analog Res-3M is demonstrated, along with its potent cytotoxicity and inhibition of microtubule dynamics.

Introduction

The ability to control the pharmacological effect of drugs using light is highly desirable for biomedical research and selective drug delivery with spatiotemporal control. This has been traditionally achieved using photolabile caging groups (Figure 1),^[1] but more recently, a new modality leveraged on photoisomerizable functional groups has emerged.^[2] This strategy predominantly makes use of the reversible isomerization of azobenzene to photoswitch the conformation of a drug. An important benefit of the photoisomerization approach over photocaging groups is that it is reversible, allowing for iterative cycling between on and off states.^[3] A prominent example of the application of this concept is the development of an azobenzene version of combretastatin A4,^[4] a high-affinity tubulin ligand with anticancer properties. In its *cis* configuration, this molecule pharmacologically mimics colchicine, a clinically used anti-proliferative agent, however, in its *trans* configuration it is inactive.^[5] Inspired by the efficiency of photocatalysis to achieve “uphill isomerization” from *trans* to *cis* by energy transfer mechanisms,^[6] and the growing range of applications of photocatalysis in chemical biology,^[7] we asked if this isomerization chemistry could be harnessed as an alternative

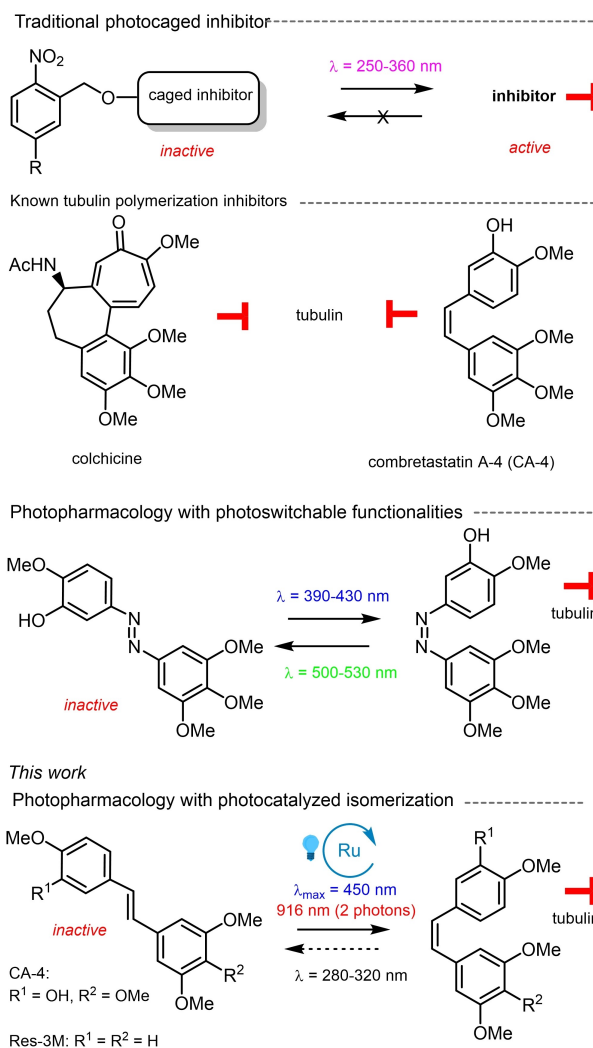


Figure 1. Scope of this work in relation to the optical control of pharmacological activity.

[*] Dr. E. E. Watson,⁺ F. Russo,⁺ Dr. D. Moreau, Prof. N. Winssinger
 Department of Organic Chemistry, NCCR Chemical Biology, Faculty
 of Sciences, University of Geneva
 1211 Geneva (Switzerland)
 E-mail: nicolas.winssinger@unige.ch

[†] These authors contributed equally to this work.

© 2022 The Authors. Angewandte Chemie International Edition published by Wiley-VCH GmbH. This is an open access article under the terms of the Creative Commons Attribution Non-Commercial License, which permits use, distribution and reproduction in any medium, provided the original work is properly cited and is not used for commercial purposes.

strategy to convert an inactive drug into an active one in a biologically relevant context. Herein we present, the use of a photocatalyst (Ru(bpy)₃Cl₂) to achieve the photoswitching on various known pharmacological agents. The present work offers the possibility to use known inhibitors without reengineering to incorporate a photoswitchable moiety as demonstrated with combretastatin A4 and other drugs. Furthermore, it confines the photoswitching to the vicinity of the catalyst, providing another dimension of selectivity by

localization or activity of the catalyst, beyond irradiation intensity.

Results and Discussion

CA-4 is derived from the African Bushwillow tree *Combretum caffrum* and was shown to inhibit tubulin formation.^[8] The clinical success of tubulin-targeting agents such as taxol and vinca alkaloids has stimulated tremendous efforts to find other inhibitors in this class. While CA-4 has demonstrated potent antiangiogenic,^[9] vascular disrupting^[10] and cytotoxic activities,^[11] its clinical development has been hampered by limited solubility (even when employing phosphate prodrugs) and confounding isomerization.^[12] Even when CA-4 is administered as the active *cis*-isomer, significant isomerization to the thermodynamically favored *trans*-isomer, which has been reported to exhibit up to a 1000-fold decrease in cytotoxicity,^[5,13] occurs and thus limits therapeutic efficacy.

While this background isomerization was detrimental to previous clinical experiments, we believed it would offer a natural off-switch in a photo-inducible system, limiting potential off-target effects resulting from accumulation of the active species. Indeed, CA-4 and its analogues have been extensively studied as potential photopharmacological agents, owing to their optically active stilbene core. While it has been demonstrated that the native CA-4 structure can undergo *trans*-to-*cis* isomerization under UV light and two-photon irradiation,^[14] the lack of biocompatibility of such conditions inspired the development of more readily isomerizable analogues, particularly those based on the azobenzene scaffolds. Trauner and Thorn-Seshold,^[4a] Streu^[4b] and Hartman^[4c] each independently explored azo-CA-4 analogues and demonstrated their utility. However, such systems are not compatible with historically useful therapeutics, requiring complete synthetic redesign, and the azo-functionality has previously demonstrated metabolic liability.^[15] Thus, we sought to develop a system in which the increased ease of photoisomerization achieved by the azo scaffold could be recapitulated without requiring synthetic modification or relying on the azo functionality.

Photocatalysis provides unique opportunities for achieving bioorthogonal transformations under mild conditions with positional control, owing to the in situ generation of the reactive species from an inert ground state catalyst.^[7,16] While both organic and transition metal complexes have been reported for the *trans* to *cis* isomerization,^[17] we reasoned that transition metal complex with a higher quantum yield for the triplet excited state would be more suitable for reaction at low concentrations (μM or below). We initiated our investigation with $\text{Ru}(\text{bpy})_3\text{Cl}_2$ based on the fact that ruthenium-based photocatalysis has been previously demonstrated in live cell and vertebrate models.^[18] Additionally, there is intense research towards the clinical development of ruthenium polypyridyl complexes for photodynamic studies.^[19] Furthermore, conjugation of the catalyst to pharmacological agents has been

shown to confine its activity to cells expressing specific receptors or subcellular compartments.^[20]

We sought to test whether uphill isomerization of *trans* to *cis* could be applied to the CA-4 scaffold using $\text{Ru}(\text{bpy})_3\text{Cl}_2$ as a photocatalyst. The relevant substrate was dissolved to a concentration of 3.2 mM in the corresponding deuterated solvent, followed by the addition of the photocatalyst as required. The ratio of *cis* to *trans* isomers was determined by NMR peak integration (Table 1, Figures S1–6). Pleasingly, upon treatment with 1 mol.% $\text{Ru}(\text{bpy})_3\text{Cl}_2$ and irradiation at 455 nm (1 W LED, 11 cm, 6.2 mW cm^{-2}) for 60 min was able to effect clean isomerization from *trans*-to-*cis*-CA-4 in a ratio of 1:9, while no conversion was observed in the absence of either light or the photocatalyst (entry 1 vs 2 and 3). However, upon further irradiation, the reaction could not be driven to completion, indicating that a slower reverse isomerization may be occurring. This hypothesis was supported by performing the same reaction starting from the *cis* isomer, which yielded a comparable ratio of isomers (entry 4 and 5), suggesting this ratio is the product of an equilibrium between a forward and backward isomerization reaction. Using riboflavin as a photocatalyst instead of $\text{Ru}(\text{bpy})_3\text{Cl}_2$ led to significantly poorer isomerization (entry 6). Interestingly, moving from DMF-d_7 to a mixture of DMSO-d_6 and D_2O significantly shifted the position of the equilibrium (entry 8), while using DMSO-d_6 alone only resulted in a small perturbation (entry 9). This behaviour is likely related to differences in relative energy of triplet states in the different solvents, therefore leading to different relative rates of isomerization in the different solvents. However, the ability to conduct this reaction in predominantly aqueous environment does demonstrate the potential for this transformation to occur in a biocompatible solvent system, and comparable conversion was also possible in cell culture media (Figure S7). Importantly, irrespective of the solvent system used, no evidence of any other chemical transformations was observed despite the presence of oxygen, suggesting that the concentration and lifetime of $^1\text{O}_2$ is insufficient to facilitate any side reactions.

We next sought to investigate the kinetics of this photocatalytic isomerization. Given our desire to apply this system to an in situ biological setting, it is vital that the

Table 1: Photocatalytic isomerization of CA-4 using 455 nm excitation.



Entry	Substrate	Solvent	Conditions	<i>trans</i> [%]	<i>cis</i> [%]
1	<i>trans</i> -CA-4	DMF-d_7	Standard	10	90
2	<i>trans</i> -CA-4	DMF-d_7	No light	> 99	< 1
3	<i>trans</i> -CA-4	DMF-d_7	No catalyst	> 99	< 1
4	<i>cis</i> -CA-4	DMF-d_7	Standard	11	89
5	<i>cis</i> -CA-4	DMF-d_7	No catalyst	< 1	> 99
6	<i>trans</i> -CA-4	DMF-d_7	1% riboflavin	84	16
7	<i>trans</i> -CA-4	DMSO-d_6	Standard	18	82
8	<i>trans</i> -CA-4	9:1 $\text{D}_2\text{O}:\text{DMSO-d}_6$	Standard	49	51

reaction proceeds at a sufficiently high rate in order to overcome the inherent limitations in concentration. The two CA-4 isomers exhibit vastly different spectral properties which we used to monitor the reaction and to identify the isomers by HPLC (Figure 2A). Using 1.25 μM of Ru(bpy)₃Cl₂ catalyst, we were able to observe the formation of the *cis* isomer within 30 s of irradiation (Figure 2B), while the reaction appeared to have reached completion within 6 min under the described conditions of irradiation in a H₂O with 7.5 % DMSO solvent mixture. By monitoring the rate of disappearance of the *trans* isomer at 329 nm (Figure 2C) we were able to extrapolate an effective pseudo-first order rate constant (Figure 2D) of $k' = 2.38 \times 10^{-3} (\pm 0.01 \times 10^{-3})$ and a corresponding second order rate constant of $1.9 \times 10^3 \text{ M}^{-1} \text{ s}^{-1}$ which is in the order of the fastest reported biorthogonal reactions (tetrazine click = $1.5 \times 10^3 - 7.3 \times 10^4 \text{ M}^{-1} \text{ s}^{-1}$).^[21] The calculated values underestimate the true rate of the forward reaction, as it reflects the rate of the net reaction progress. It should be noted that, while the reaction could be pushed to near completion in DMF, the reaction was significantly slower, taking nearly 2 h (see Figure S8 for quantification) which is consistent with the NMR observations. The rate could be increased by the use of more intense light sources but our investigations were limited to 1 W LED (6.2 mW cm^{-2}) which has been shown to be compatible with the irradiation of live cells or organisms.^[18b]

We next sought to determine whether this conversion was unique to CA-4 or could be applied to other alkene containing substrates. Initially we explored the related stilbene natural products *trans*-resveratrol trimethyl ether (*trans*-Res-3M, also known as trimethoxystilbene (TMS)) and pterostilbene and were pleased to see that smooth conversion was achieved on a similar time scale (Figure 3, S9–S14). Buoyed by this observation we sought to test whether a broader substrate scope could be exploited. To this end, we tested a range of commercially available therapeutic agents containing a range of alkene functionalities. We were pleased to see that the conversion occurred smoothly on both electron rich and electron poor alkenes, and the presence of heterocycles was also well tolerated. Importantly, the transformation was not limited to substrates containing the stilbene core. Indeed, Mubrutinib, CNB-001 and QNZ-46 all converted smoothly within 30 min in spite of the presence of a conjugated heteroaromatic core (Figure S15–S24).

Taken together, the results indicate that isomerization of diverse pharmacophores towards the thermodynamically unfavored isomer using low concentrations (μM) and catalyst loading (1 %) is possible on a timescale that is applicable to biological setting (30 min) in a light flux dependent manner (6.2 mW cm^{-2} , see Figure S25 for reactions performed at lower light intensity).

We next explored whether the Ru-mediated photocatalytic isomerization could recapitulate the phenotypic activity of a native *cis*-containing molecule. In addition to CA-4, we chose to evaluate *trans*-Res-3M, a naturally occurring resveratrol analogue that has been shown to be well tolerated at high concentrations in vivo reaching a plasma concentration of $> 80 \mu\text{M}$ with oral administration.^[22]

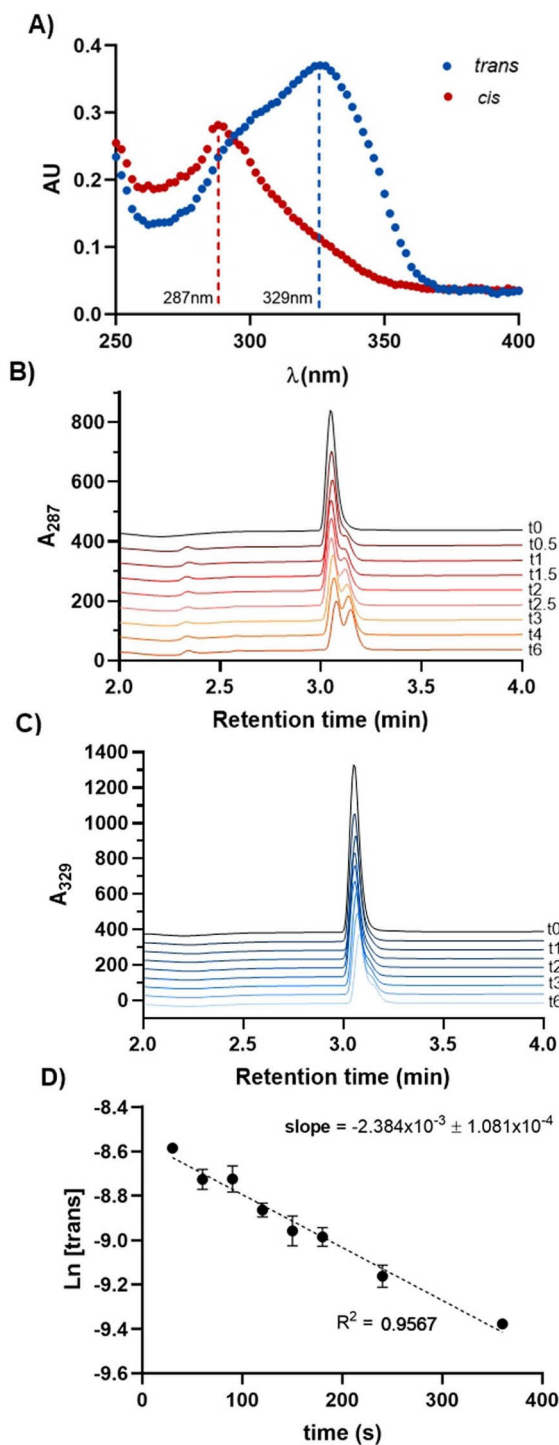


Figure 2. Rate of photocatalytic isomerization of CA-4. *Trans*-CA-4 was prepared as a 3.2 mM stock in DMSO and diluted in water to a final concentration of 250 μM (7.5 % DMSO final concentration), containing 1.25 μM Ru(bpy)₃Cl₂. A) The absorption maximum was determined for each isomer; B) and C) the reaction progression (t in min) was monitored at each wavelength by triplicate injection on reversed-phase HPLC. D) Remaining concentration of the *trans* isomer was calculated as a function of the absorbance of the pure *cis* and *trans* isomers at 329 nm, with the natural log taken to arrive at the pseudo-first order rate constant. Error bars represent standard deviation.

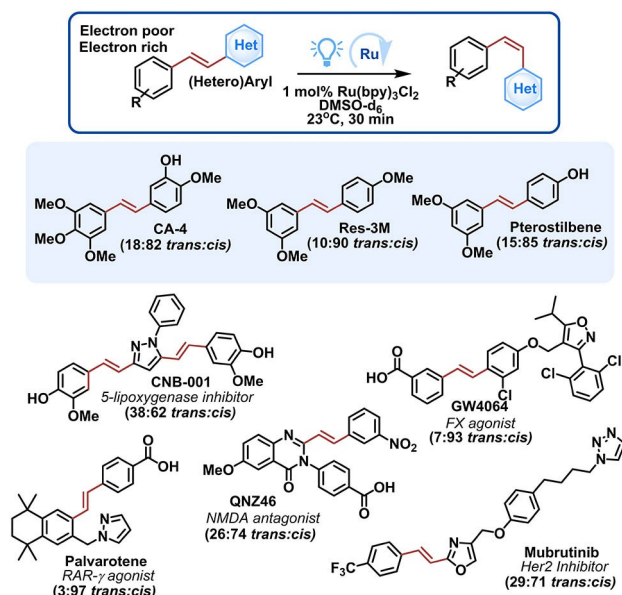


Figure 3. Substrate scope for photocatalytic isomerization amongst therapeutically relevant molecules. Experiment conducted at 3.2 mM substrate. *Trans* to *cis* ratio determined by integration of NMR peaks (see Figure S9–24 for NMR quantifications and LC-MS characterizations).

Importantly, its *cis* isomer (*cis*-Res-3M) has also been reported to exert similar antiproliferative activity to combretastatin (tubulin inhibition and antiproliferative effect), albeit with lower potency.^[23] Initially, we evaluated both compounds in terms of their effect on microtubule dynamics. To do this we employed a HeLa cell line stably expressing (under antibiotic selection) GFP-EB3,^[24] a protein which associates with the growing end of the microtubule.^[25] The accumulation of EB3 at dynamic end results in so-called “comets” that can be quantified in terms of number, size and speed as a reflection of any perturbation to the native microtubule network (Figure 4A). Pleasingly, we were able to observe a significant increase in potency of microtubule disruption for each of the compounds upon photoisomerization as compared to the *trans* isomer.

Briefly, GFP-EB3 HeLa cells were treated with either the *trans*-isomer or a pre-isomerized solution of CA-4, with both conditions containing the same amount of catalyst (Figure 3B) and Res-3M (Figure 3C), respectively, for 15 min before determination of the comet number by automated microscopy (see Supporting Information for full experimental details, Figure S26–S30). The difference between the isomerized sample and *trans* isomers was clearly observable in the comet analysis (IC₅₀ of 11.9 nM for isomerized-CA-4 vs 7378 nM for the *trans*-CA-4; IC₅₀ of 259 nM for isomerized-Res-3M vs > 50 μM for the *trans*-Res-3M) as well as in a cell viability assay where 20 h treatment led to cytotoxicity at 50 nM for the *isomerized*-Res-3M, whereas no cytotoxicity is observed at 50 μM for the *trans*-Res-3M (Figure 4D, Figure S31 for in situ isomerization). Using an assay for caspase-3/7 activity (fluorogenic substrate) as a marker of apoptosis, we also demonstrated

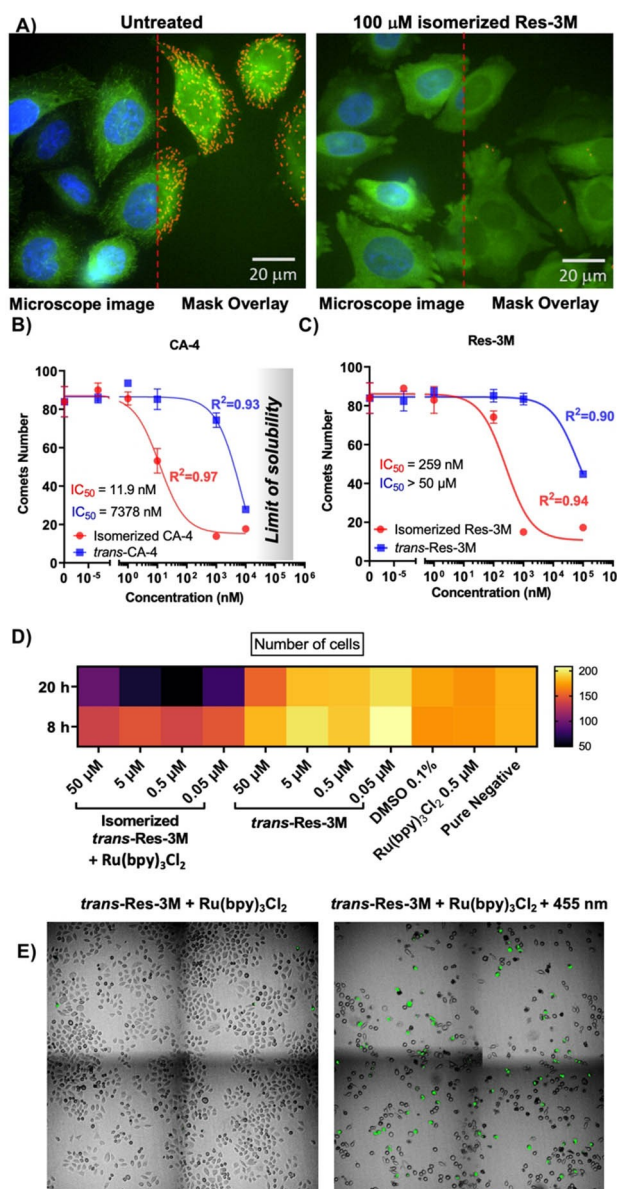


Figure 4. Phenotypic effects of photoisomerized stilbenes. A) representative images (microscope image, left, and comet identifying mask, right (separated by red line)) and IC₅₀ curves for disruption of microtubule dynamics for the parent *trans* and photoisomerized variants of B) CA-4 and C) Res-3M. In vitro photoisomerization of *trans*-Res-3M is also able to induce D) cytotoxicity (as demonstrated in a nuclear count assay) and E) apoptosis (measured by caspase 3/7 activity, green represents activity). Expanded version of (E) with additional controls is provided in Figure S32). For all experiments photoisomerization was conducted in DMSO at 10 mM (CA-4) or 50 mM (Res-3M) with 1 mol.% Ru(bpy)₃Cl₂ and irradiated prior to addition to cell at 455 nm for 30 min which provides *trans:cis* ratios of 18:82 and 10:90, respectively.

that the cytotoxicity of the isomerized sample is indeed the result of apoptosis (Figure 4E) whereas the *trans* isomer in combination with the catalyst did not induce any measurable apoptosis relative to a DMSO control (Figure 4E, see Figure S32 for additional controls with *trans* isomer, photo-

catalyst and irradiation). Given the lower toxicity of the *trans* isomer of Res-3M compared to CA-4, the preponderance of resveratrol derivatives in food and the established tolerability of *trans*-Res-3M, we chose to continue our studies with this analogue for *in cellulo* experiments.

Following our demonstration that phenotypic differences could be observed between the *trans*- and photoisomerized Res-3M, we next sought to evaluate whether we could achieve *in situ* isomerization and activation of Res-3M. We chose to use the EB3-GFP labelled system given the real-time readout and sensitivity to small perturbations in microtubule dynamics. HeLa cells stably expressing EB3-GFP (under antibiotic selection) were incubated with 5 μM Res-3M and 0.05 μM Ru(bpy)₃Cl₂ and irradiated for 180 seconds at 455 nm (Figure 5). Pleasingly, a stark decrease in the number of comets was observed in the treatment group, while all other combinations of the treatment conditions showed no effects.

A key limitation of blue light-mediated photopharmacology platforms is the inherent poor tissue penetration (typically ≤ 0.2 cm)^[26] which hampers potential clinical application. One key way in which this can be overcome is through the use of two-photon irradiation. This affords equivalent energy transitions through rapid, sequential

absorption of two lower energy (and thus more penetrating) photons by the same molecule. Thus, we sought to explore whether two-photon excitation could also be applied to our system. Once again, EB3-GFP HeLa cells were treated with 5 μM Res-3M (with or without the presence of 10 μM Ru(bpy)₃Cl₂) and irradiated with a 916 nm two-photon laser over a period of 3 minutes (Figure 6, S33–S35). Within 50 s of irradiation a significant decrease was once again observed in the number of comets (with complete disappearance observed within 125 s) while the treatment group lacking the photocatalyst remained unchanged throughout the course of the experiment. Significantly, these conditions did not lead to the formation of detectable levels of singlet oxygen from the Ru(bpy)₃Cl₂ photocatalyst using a fluorescent dye (Si-DMA)^[27] responsive to ¹O₂. While Ru(bpy)₃Cl₂ is known to sensitize the formation of ¹O₂, the results indicate that at the catalyst loading and irradiation power, the cellular redox buffer is sufficient to quench the ¹O₂ generated (see Supporting Information Figures S36 and S37).

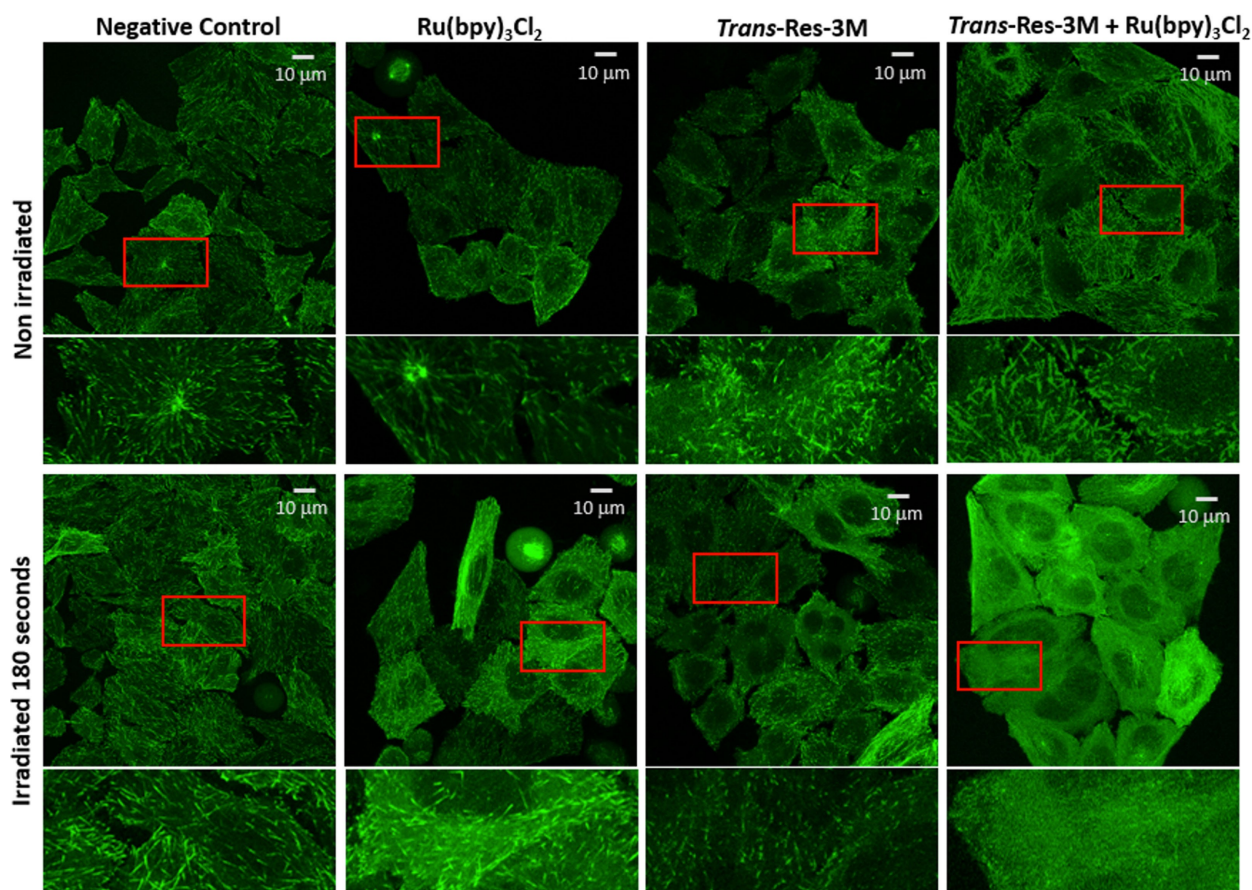


Figure 5. *In situ* photoisomerization of *trans*-Res-3M disrupts microtubule dynamics. EB3-GFP HeLa cells were incubated with 5 μM *trans*-Res-3M, 0.05 μM Ru(bpy)₃Cl₂ and irradiated with an LED light for 180 s at 455 nm. Red boxes indicate the areas corresponding to the expansions shown below each image.

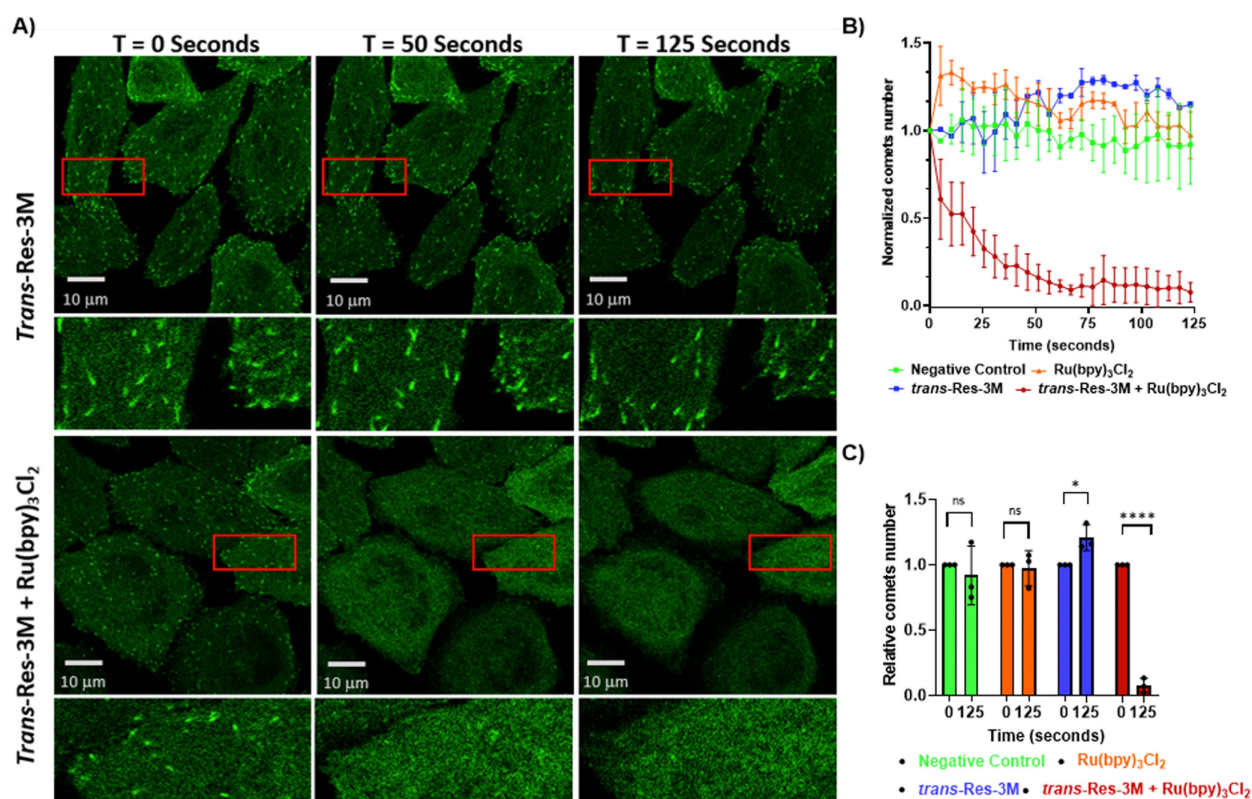


Figure 6. Perturbation of microtubule dynamics occurs within 50 s using two-photon irradiation at 916 nm to photoisomerize *trans*-Res-3M in situ. E3B-GFP HeLa cells were incubated 10 μM of $\text{Ru}(\text{bpy})_3\text{Cl}_2$ for 3 hours. After extensive washing cells were treated with 5 μM *trans*-Res-3M and irradiated for 180 s at 916 nm. A) Raw time course images for cells (and expansions corresponding to the areas indicated in red boxes, below) in the presence or absence of $\text{Ru}(\text{bpy})_3\text{Cl}_2$ and quantification of B) time course and C) endpoint comet number (see Figure S25 for images corresponding to catalyst alone or pure negative). *P* values ≤ 0.05 denoted as *, *P* values ≤ 0.0001 denoted as ****. See videos 1 and 2 for a time-lapse of shown conditions (*trans*-Res-3M + $\text{Ru}(\text{bpy})_3\text{Cl}_2$ or *trans*-Res-3M alone respectively). Expanded version of A) containing all relevant controls is provided in the Supporting Information Figures S33.

Conclusion

In summary, we have demonstrated a mild and biocompatible means of undertaking photocatalyzed geometric isomerization of a range of therapeutically relevant compounds. Not only does this provide exciting opportunities for in situ activation of therapeutic agents with enhanced selectivity due to the spatio- and temporal control afforded by irradiation, but also the potential to enhance this through photocatalyst localization to target cell subtypes. For CA-4, the rate of photocatalyzed isomerization was $1.9 \times 10^3 \text{ M}^{-1} \text{ s}^{-1}$ at moderate irradiation intensity (1 W LED lamp, 6.2 mW cm^{-2}), enabling the reaction to proceed at low substrate concentration and low catalyst loading. Given the simple and rapid nature of the reaction, in addition to its functional group tolerance, one may envisage incorporating such isomerization reactions into the biological screening of alkene containing compound collection. The paucity of drugs with a *cis*-stilbene motif is not surprising considering the isomeric instability of the *cis*-alkene. In fact, this isomerization has been an issue in the development of combretastatin. Furthermore, the *trans* to *cis* isomerization reaction described herein could also be used in designer molecule where the stilbene moiety does not necessarily participate

directly into the binding but merely acts as a steric discrimination, enabling drug binding in the *cis* configuration and precluding drug binding in the *trans*. This strategy would allow the stilbene moiety to be tuned electronically to the most suitable isomerization configurations. The reaction could also be used to alter the conformation of stapled peptides (*i* and *i* + 7). While the screening of isomerization of the different bioactive compounds indicates a broad scope, the *cis/trans* ratio obtained at equilibrium varied. It is possible that tuning the photocatalyst's triplet energy level in order to achieve a more selective energy transfer to the *trans* vs. *cis* isomer could be used to optimize the ratio obtained. However, this point is less important if the bioactive compound is the thermodynamically unfavored isomer and there is a broad therapeutic window between the *cis* and *trans* isomers, as is the case for CA-4 and Res-3M. It should be noted that azobenzene photoswitch also displays a variable *cis-trans* isomerization ratio. The salient feature of this chemistry is the fast kinetic of the photocatalyzed reaction at biologically tolerated irradiation. This is by virtue of the efficiency of the energy transfer mechanism. While the photoredox properties of transition metals are increasingly used in chemical biology, there is only one example of a Dexter energy transfer reported to activate a diazirine

cross linker.^[28] The application of an energy transfer to effect an isomerization is yet another example of the application of photocatalysis in chemical biology and therapeutic ends.

Experimental Section

Experimental procedures, characterization data, spectroscopic data and microscopy data can be found in the attached Supporting Information file. The raw data have been deposited on Zenodo <https://doi.org/10.5281/zenodo.6542168>

Acknowledgements

This work was supported by the Swiss National Science Foundation (188406), NCCR Chemical Biology (185898), EMBO (postdoctoral fellowship ALTF 1015-2020 to EEW). We thank Prof. Meraldi (University of Geneva, Department of cell physiology and metabolism, CMU) for the E3B-GFP expressing HeLa cell line used in this study. We thank Christoph Bauer from the Bioimaging center, University of Geneva for his technical assistance with microscopy. Open access funding provided by Universite de Geneve.

Conflict of Interest

The authors declare no conflict of interest.

Data Availability Statement

The data that support the findings of this study are available in the Supporting Information of this article.

Keywords: Optochemistry · Photocatalysis · Photoisomerization · Photopharmacology · Tubulin Binder

- [1] N. Ankenbruck, T. Courtney, Y. Naro, A. Deiters, *Angew. Chem. Int. Ed.* **2018**, *57*, 2768–2798; *Angew. Chem.* **2018**, *130*, 2816–2848.
- [2] a) J. Broichhagen, J. A. Frank, D. Trauner, *Acc. Chem. Res.* **2015**, *48*, 1947–1960; b) K. Hüll, J. Morstein, D. Trauner, *Chem. Rev.* **2018**, *118*, 10710–10747; c) W. A. Velema, W. Szymanski, B. L. Feringa, *J. Am. Chem. Soc.* **2014**, *136*, 2178–2191; d) Z. L. Pianowski, *Chem. Eur. J.* **2019**, *25*, 5128–5144; e) A. Müller-Deku, J. C. M. Meiring, K. Loy, Y. Kraus, C. Heise, R. Bingham, K. I. Jansen, X. Qu, F. Bartolini, L. C. Kapitein, A. Akhmanova, J. Ahlfeld, D. Trauner, O. Thorn-Seshold, *Nat. Commun.* **2020**, *11*, 4640; f) A. Sailer, J. C. M. Meiring, C. Heise, L. N. Pettersson, A. Akhmanova, J. Thorn-Seshold, O. Thorn-Seshold, *Angew. Chem. Int. Ed.* **2021**, *60*, 23695–23704; *Angew. Chem.* **2021**, *133*, 23888–23897.
- [3] M.-M. Russew, S. Hecht, *Adv. Mater.* **2010**, *22*, 3348–3360.
- [4] a) M. Borowiak, W. Nahaboo, M. Reynders, K. Nekolla, P. Jalintot, J. Hasserodt, M. Rehberg, M. Delattre, S. Zahler, A. Vollmar, D. Trauner, O. Thorn-Seshold, *Cell* **2015**, *162*, 403–411; b) A. J. Engdahl, E. A. Torres, S. E. Lock, T. B. Engdahl, P. S. Mertz, C. N. Streu, *Org. Lett.* **2015**, *17*, 4546–4549; c) J. E. Sheldon, M. M. Dcona, C. E. Lyons, J. C. Hackett, M. C. T. Hartman, *Org. Biomol. Chem.* **2016**, *14*, 40–49.
- [5] R. Gaspari, A. E. Prota, K. Bargsten, A. Cavalli, M. O. Steinmetz, *Chem* **2017**, *2*, 102–113.
- [6] F. Strieth-Kalthoff, M. J. James, M. Teders, L. Pitzer, F. Glorius, *Chem. Soc. Rev.* **2018**, *47*, 7190–7202.
- [7] W. Liu, E. E. Watson, N. Winssinger, *Helv. Chim. Acta* **2021**, *104*, e2100179.
- [8] a) G. R. Pettit, S. B. Singh, M. R. Boyd, E. Hamel, R. K. Pettit, J. M. Schmidt, F. Hogan, *J. Med. Chem.* **1995**, *38*, 1666–1672; b) G. R. Pettit, S. B. Singh, E. Hamel, C. M. Lin, D. S. Alberts, D. Garciakendall, *Experientia* **1989**, *45*, 209–211.
- [9] J. Griggs, R. Hesketh, G. A. Smith, K. M. Brindle, J. C. Metcalfe, G. A. Thomas, E. D. Williams, *Br. J. Cancer* **2001**, *84*, 832–835.
- [10] a) A. Gaya, F. Daley, N. J. Taylor, G. Tozer, U. Qureshi, A. Padhani, R. B. Pedley, R. Begent, D. Wellsted, J. J. Stirling, G. Rustin, *Br. J. Cancer* **2008**, *99*, 321–326; b) W. Landuyt, O. Verdoes, D. O. Darius, M. Drijkoningen, S. Nuyts, J. Theys, L. Stockx, W. Wynendaale, J. F. Fowler, G. Maleux, W. Van den Bogaert, J. Anné, A. van Oosterom, P. Lambin, *Eur. J. Cancer* **2000**, *36*, 1833–1843.
- [11] a) C.-H. Shen, J.-J. Shee, J.-Y. Wu, Y.-W. Lin, J.-D. Wu, Y.-W. Liu, *Br. J. Pharmacol.* **2010**, *160*, 2008–2027; b) D. Simoni, R. Romagnoli, R. Baruchello, R. Rondanin, M. Rizzi, M. G. Pavani, D. Alloatti, G. Giannini, M. Marcellini, T. Riccioni, M. Castorina, M. B. Guglielmi, F. Bucci, P. Carminati, C. Pisano, *J. Med. Chem.* **2006**, *49*, 3143–3152; c) J. Griggs, J. C. Metcalfe, R. Hesketh, *Lancet Oncol.* **2001**, *2*, 82–87.
- [12] C. J. Mooney, G. Nagaiah, P. Fu, J. K. Wasman, M. M. Cooney, P. S. Savvides, J. A. Bokar, A. Dowlati, D. Wang, S. S. Agarwala, S. M. Flick, P. H. Hartman, J. D. Ortiz, P. N. Lavertu, S. C. Remick, *Thyroid* **2009**, *19*, 233–240.
- [13] a) G. R. Pettit, M. R. Rhodes, D. L. Herald, D. J. Chaplin, M. R. L. Stratford, E. Hamel, R. K. Pettit, J.-C. Chapuis, D. Oliva, *Anti-Cancer Drug Des.* **1998**, *13*, 981–993; b) G. R. Pettit, M. R. Rhodes, D. L. Herald, E. Hamel, J. M. Schmidt, R. K. Pettit, *J. Med. Chem.* **2005**, *48*, 4087–4099.
- [14] a) K. Scherer, R. Bisby, S. Botchway, J. Hadfield, A. Parker, *J. Biomed. Opt.* **2014**, *20*, 051004; b) R. H. Bisby, S. W. Botchway, G. M. Greetham, J. A. Hadfield, A. T. McGown, A. W. Parker, K. M. Scherer, M. Towrie, *Meas. Sci. Technol.* **2012**, *23*, 084001; c) Hadfield, A. T. McGown, S. P. Mayalarp, E. J. Land, I. Hamblett, K. Gaukroger, N. J. Lawrence, L. A. Hepworth, J. Butler, WO200250007, **2002**.
- [15] a) A. A. Beharry, O. Sadoski, G. A. Woolley, *J. Am. Chem. Soc.* **2011**, *133*, 19684–19687; b) S. Samanta, C. Qin, A. J. Lough, G. A. Woolley, *Angew. Chem. Int. Ed.* **2012**, *51*, 6452–6455; *Angew. Chem.* **2012**, *124*, 6558–6561; c) L. Gao, J. C. M. Meiring, Y. Kraus, M. Wranik, T. Weinert, S. D. Pritzl, R. Bingham, E. Ntoulou, K. I. Jansen, N. Olieric, J. Standfuss, L. C. Kapitein, T. Lohmüller, J. Ahlfeld, A. Akhmanova, M. O. Steinmetz, O. Thorn-Seshold, *Cell Chem. Biol.* **2021**, *28*, 228–241.e226.
- [16] J. Twilton, C. Le, P. Zhang, M. H. Shaw, R. W. Evans, D. W. C. MacMillan, *Nat. Chem. Rev.* **2017**, *1*, 0052.
- [17] a) K. Singh, S. J. Staig, J. D. Weaver, *J. Am. Chem. Soc.* **2014**, *136*, 5275–5278; b) J. B. Metternich, D. G. Artiukhin, M. C. Holland, M. von Bremen-Kühne, J. Neugebauer, R. Gilmour, *J. Org. Chem.* **2017**, *82*, 9955–9977; c) W. Cai, H. Fan, D. Ding, Y. Zhang, W. Wang, *Chem. Commun.* **2017**, *53*, 12918–12921; d) L. Schmid, C. Kerzig, A. Prescimone, O. S. Wenger, *JACS Au* **2021**, *1*, 819–832.
- [18] a) J. Y. Lee, D. G. Udugamasooriya, H. S. Lim, T. Kodadek, *Nat. Chem. Biol.* **2010**, *6*, 258–260; b) L. Holtzer, I. Oleinich, M. Anzola, E. Lindberg, K. K. Sadhu, M. Gonzalez-Gaitan, N. Winssinger, *ACS Cent. Sci.* **2016**, *2*, 394–400; c) K. K. Sadhu, T.

- Eierhoff, W. Romer, N. Winssinger, *J. Am. Chem. Soc.* **2012**, *134*, 20013–20016.
- [19] F. Heinemann, J. Karges, G. Gasser, *Acc. Chem. Res.* **2017**, *50*, 2727–2736.
- [20] a) K. K. Sadhu, E. Lindberg, N. Winssinger, *Chem. Commun.* **2015**, *51*, 16664–16666; b) M. Martínez-Alonso, G. Gasser, *Coord. Chem. Rev.* **2021**, *434*, 213736.
- [21] E. J. L. Stéen, J. T. Jørgensen, C. Denk, U. M. Battisti, K. Nørregaard, P. E. Edem, K. Bratteby, V. Shalgunov, M. Wilkovitsch, D. Svatunek, C. B. M. Poulie, L. Hvass, M. Simón, T. Wanek, R. Rossin, M. Robillard, J. L. Kristensen, H. Mikula, A. Kjaer, M. M. Herth, *ACS Pharmacol. Transl. Sci.* **2021**, *4*, 824–833.
- [22] H. S. Lin, P. C. Ho, *J. Pharm. Sci.* **2011**, *100*, 4491–4500.
- [23] a) P. Chabert, A. Fougèrousse, R. Brouillard, *BioFactors* **2006**, *27*, 37–46; b) C. B. Nguyen, H. Kotturi, G. Waris, A. Mohammed, P. Chandrakesan, R. May, S. Sureban, N. Weygant, D. Qu, C. Rao, D. N. Dhanasekaran, M. S. Bronze, C. W. Houchen, N. Ali, *Cancer Res.* **2016**, *76*, 4887–4896; c) Y. Schneider, P. Chabert, J. Stutzmann, D. Coelho, A. Fougèrousse, F. Gosse, J. F. Launay, R. Brouillard, F. Raul, *Int. J. Cancer* **2003**, *107*, 189–196; d) G. R. Pettit, M. P. Grealish, M. K. Jung, E. Hamel, R. K. Pettit, J. C. Chapuis, J. M. Schmidt, *J. Med. Chem.* **2002**, *45*, 2534–2542.
- [24] J. W. Armond, E. Vladimirov, M. Erent, A. D. McAinsh, N. J. Burroughs, *J. Cell Sci.* **2015**, *128*, 1991–2001.
- [25] a) P. Bieling, L. Laan, H. Schek, E. L. Munteanu, L. Sandblad, M. Dogterom, D. Brunner, T. Surrey, *Nature* **2007**, *450*, 1100–1105; b) Sebastian P. Maurer, Franck J. Fourniol, G. Bohner, Carolyn A. Moores, T. Surrey, *Cell* **2012**, *149*, 371–382; c) T. Stepanova, J. Slemmer, C. C. Hoogenraad, G. Lansbergen, B. Dortmund, C. I. De Zeeuw, F. Grosveld, G. van Cappellen, A. Akhmanova, N. Galjart, *J. Neurosci.* **2003**, *23*, 2655–2664.
- [26] C. Ash, M. Dubec, K. Donne, T. Bashford, *Lasers Med. Sci.* **2017**, *32*, 1909–1918.
- [27] S. Kim, T. Tachikawa, M. Fujitsuka, T. Majima, *J. Am. Chem. Soc.* **2014**, *136*, 11707–11715.
- [28] J. B. Geri, J. V. Oakley, T. Reyes-Robles, T. Wang, S. J. McCarver, C. H. White, F. P. Rodriguez-Rivera, D. L. Parker, E. C. Hett, O. O. Fadeyi, R. C. Oslund, D. W. C. MacMillan, *Science* **2020**, *367*, 1091–1097.

Manuscript received: March 4, 2022

Accepted manuscript online: May 4, 2022

Version of record online: May 20, 2022